Recent Results on Charm Photoproduction

Don Hochman*
On behalf of the ZEUS Collaboration

*Weizmann Institute of Science, Rehovot Israel 76100

Abstract. Photoproduction of $D_s^{\pm}$ mesons has been measured in the ZEUS detector at HERA and compared with predictions of NLO pQCD calculations. The ratio of $D_s^{*\pm}$ to $D^{*\pm}$ cross sections has been compared to results from e^+e^- experiments. Orbitally excited P-wave charm mesons have been observed in the $D^{*\pm}\pi^{\mp}$ final state. The fraction of $D^{*\pm}$'s originating from these mesons has been calculated and compared with that from e^+e^- interactions. No evidence for radially excited mesons decaying to $D^{*\pm}\pi^+\pi^-$ was found. The inelastic production of J/ψ mesons has been measured and compared to LO and NLO pQCD predictions.

INTRODUCTION

Charm photoproduction measurements have been performed at the HERA ep collider in the ZEUS detector from data taken during 1995-2000. Electrons or positrons with energy $E_e = 27.5\,GeV$ collided with protons of energy $E_p = 820\,GeV$ (1995-1997) or $E_p = 920\,GeV$ (1998-2000). The ZEUS detector description can be found elsewhere [1].

The decay chain $D_s{}^{\pm} \to \phi\pi^{\pm} \to K^+K^-\pi^{\pm}$ (38pb^{-1} integrated luminosity) was studied [2] as a continuation of a previous analysis of charm photoproduction [3]. The study of $D_s^{\pm}$ photoproduction provides another test of next-to-leading order (NLO) perturbative quantum chromodynamics (pQCD) calculations.

Orbitally excited P-wave D mesons can decay to a D^* by pion emission. Two of these states ($D_1(2420)$ and $D_2^*(2460)$) have been found to decay into narrow states [4] with properties predicted by Heavy Quark Effective Theory (HQET) [5] and a third broad state has been seen by the CLEO collaboration [6]. A radial excitation of the $D^{*\pm}$ with a mass of about 2.6 GeV decaying into $D^{*\pm}\pi^+\pi^-$ has been reported by DELPHI [7] but not seen by OPAL and CLEO [8,9].

Inelastic J/ψ photoproduction proceeds via direct (resolved) processes, where the virtual photon (parton from the photon) interacts with a parton from the incoming proton. In the dominant process, boson gluon fusion (BGF), the latter parton is a gluon. Photon diffraction to J/ψ also contributes. The inelasticity variable,

$z = \frac{P \cdot p_\psi}{P \cdot q}$, can be used to distinguish these processes. Here P, p_ψ and q are the four-momenta of the incoming proton, J/ψ and exchanged photon, respectively. From previous ZEUS data [10] the diffractive process dominates at $z > 0.9$, the direct photon process dominates at $0.4 < z < 0.9$. The resolved photon contribution is expected to dominate at $z \lesssim 0.2$ [11].

Color singlet and color octet models have been used to calculate the above non-diffractive production processes in pQCD. For the former, the charm-anticharm pair ($c\bar{c}$) from the hard process is identified with the physical J/ψ state. In this model in leading order (LO) only the BGF diagram contributes to the direct channel. In the color octet model the $c\bar{c}$ pair from the hard process emits one or more soft gluons to evolve into the physical J/ψ state. The free parameters of the model can be extracted from J/ψ cross-section measurements and used in other inelastic J/ψ production experiments.

$D_S^{\pm}$ PHOTOPRODUCTION

$D_s^{\pm}$ production was studied for: $Q^2 < 1.0\,GeV^2$,$130 < W_{\gamma p} < 280\,GeV$,$3 < p_\perp^{D_s} < 12\,GeV$, $|\eta^{D_s}| < 1.5$, where Q^2 is the photon virtuality, $W_{\gamma p}$ is the virtual photon proton center of mass energy, $p_\perp^{D_s}$ is the transverse momentum of the $D_s^{\pm}$ and η^{D_s} is the pseudorapidity of the $D_s^{\pm}$. The effective mass of two opposite charge track combinations, assumed to be kaons, was calculated and plotted in Fig. 1a. A clear enhancement at the ϕ mass is seen. The effective mass of the combinations in this enhancement region and another track assumed to be a pion was then obtained. The peak in the $D_s^{\pm}$ mass region contained 339 ± 48 $D_s^{\pm}$ mesons (Fig. 1b), corresponding to a cross section of $\sigma_{ep \to D_s X} = 3.79 \pm 0.59(stat)^{+0.26}_{-0.46}(syst) \pm 0.94(br)\,nb$.

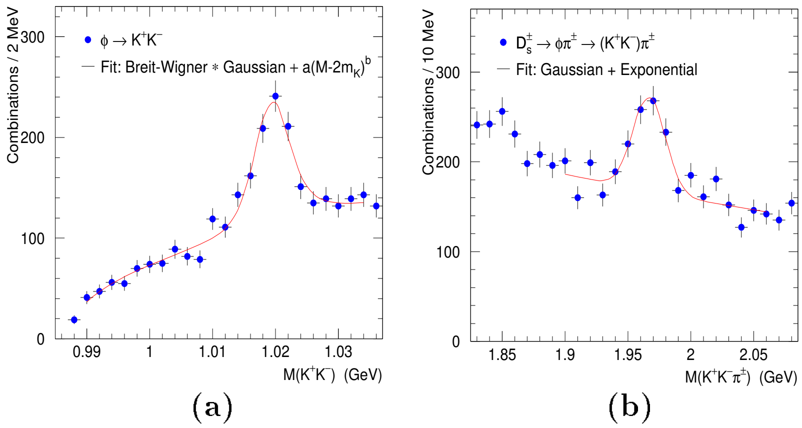

FIGURE 1. (a) $M(K^+K^-)$ distribution for events inside the $D_s^{\pm}$ mass range, $(1.94 < M(K^+K^-\pi^{\pm}) < 2.00\,GeV)$. The solid curve is a fit to a Breit-Wigner convoluted with a Gaussian-shaped resonance and a background parameterization, $a[M(K^+K^-) - 2m_K]^b$. (b) $M(K^+K^-\pi^{\pm})$ distribution for events in the ϕ mass range, $(1.0115 < M(K^+K^-) < 1.0275\,GeV)$. The solid curve is a fit to a Gaussian plus an exponential background.

Distributions in $p_\perp^{D_s}$ and η^{D_s} were compared with those for $D^{*\pm}$ production [3] and with a fixed order NLO calculation [12] in which charm was produced by the BGF process. The signal is above the prediction (Fig. 2), particularly for η along the proton beam direction, as was the case for $D^{*\pm}$ production.

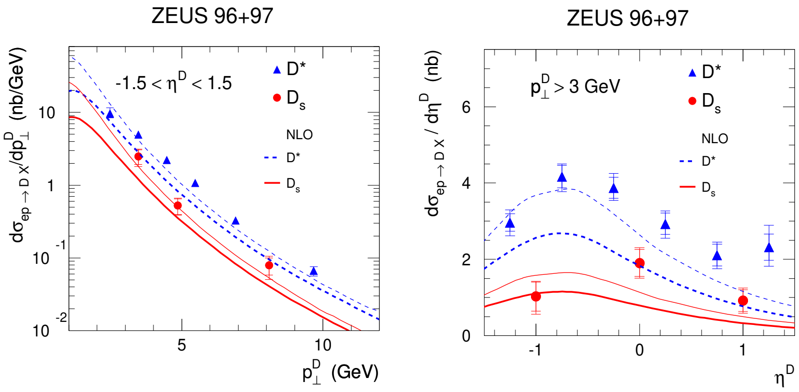

(a) (b)

FIGURE 2. Differential cross sections for the photoproduction reaction $ep \to DX$: (a) $d\sigma/dp_\perp^D$ and (b) $d\sigma/d\eta^D$, where D stands for D^* or D_s. Inner (outer) error bars show statistical (statistical and systematic added in quadrature) errors. The D_s (dots) and D^* (triangles) data are compared with NLO predictions for D_s (full curves) and D^* (dashed curves) with two parameter settings: $m_c = 1.5\,GeV$, $\mu_R = m_\perp$ (thick curves) and $m_c = 1.2\,GeV$, $\mu_R = 0.5 m_\perp$ (thin curves).

The ratio of the cross section for $D_s^\pm$ to $D^{*\pm}$ production at HERA has been compared to that from e^+e^- experiments, where the latter result is taken from a recent compilation [13] of fragmentation fractions to charm mesons ($f(c \to D)$). The results from the two types of interactions are:
$\sigma_{ep\to D_s X}/\sigma_{ep\to D^* X} = 0.41 \pm 0.07^{+0.03}_{-0.05}$ and $f(c \to D_s^+)/f(c \to D^{*+}) = 0.43 \pm 0.04$.
The strangeness suppression factor, γ_s, (the ratio of the probability to produce a strange quark to that to produce a non-strange quark), has also been compared to that from e^+e^- experiments. From HERA the value of the above cross section ratio and the PYTHIA Monte Carlo was used and for e^+e^- the quantity $2f(c \to D_s^+)/[f(c \to D^0) + f(c \to D^+)]$ served as an estimator for γ_s. The values of γ_s for HERA and e^+e^-, respectively, were $0.27 \pm 0.04^{+0.02}_{-0.03}$ and 0.26 ± 0.03, implying consistency with universal charm fragmentation.

EXCITED CHARM MESONS

As a basis for the study of higher excitatations of charm mesons, an enlarged sample of data (integrated luminosity of $110 \mathrm{pb}^{-1}$), containing a clean signal of $D^{*\pm}$ mesons from both photoproduction and deep inelastic scattering, was used [14]. Events in the mass range $1.83 < M(K\pi) < 1.90\,GeV$, $0.144 < M(K\pi\pi_s) - M(K\pi) < 0.147\,GeV$ were chosen (π_s is the low momentum pion in the D^* decay).

The background (estimated from events in which the K and π in the D^0 mass range have the same charge) has been subtracted, yielding 27286 ± 232 $D^{*\pm}$.

For orbital excitations an extra track, π_4, was added to the $D^{*\pm}$ candidate and the effective mass combination, $M(K\pi\pi_s\pi_4) - M(K\pi\pi_s) + M(D^*)(2.010\,GeV)$, was evaluated. An enhancement in the mass distribution with total charge zero is seen in Fig. 3a. This spectrum was fitted to D_1^0 and D_2^{*0} Breit-Wigner shapes with masses and widths fixed [4], and convoluted with a Gaussian function with a width as in the Monte Carlo simulation. The background was described by $x^\alpha e^{-\beta x + \gamma x^2}$, where $x = M(K\pi\pi_s\pi_4) - M(K\pi\pi_s) - m_\pi$, with α, β and γ constant. Helicity angle distributions for D_1^0 and D_2^{*0} proportional to $1 + 3\cos^2\theta$ and $1 - \cos^2\theta$, respectively, were folded in for the fit. Here, θ is the angle between π_4 and π_s in

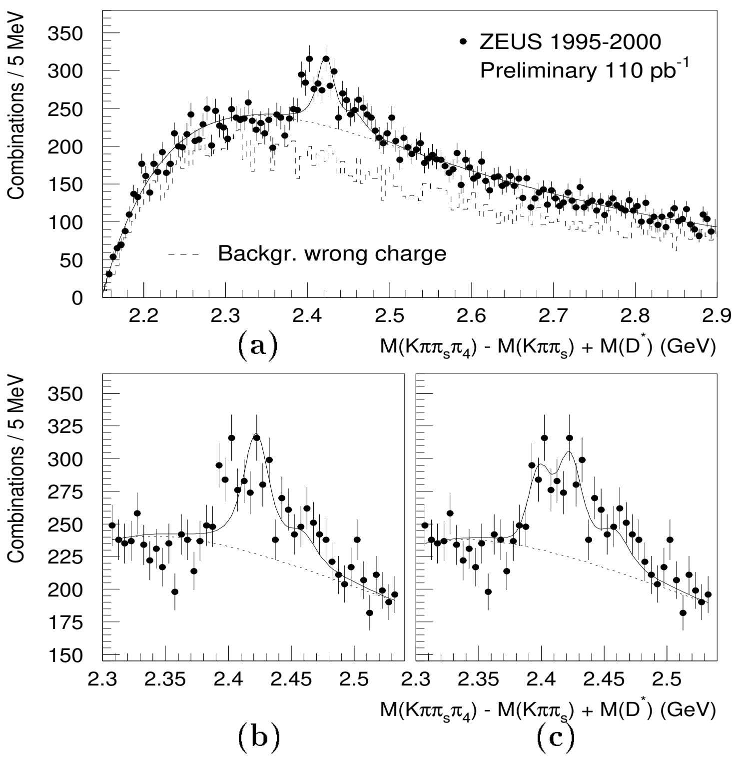

FIGURE 3. Distribution of $M(K\pi\pi_s\pi_4) - M(K\pi\pi_s) + M(D^*)(2.010\,GeV)$ for D^* and π_4 with opposite charges. (a)-(b) Fit to two Breit-Wigner shapes convoluted with a Gaussian (full curve). The dashed histogram is for D^* and π_4 with the same charge. (c) Fit included extra Gaussian with free mass and width. The dotted curves are the fitted combinatorial background.

the $D^{*\pm}$ rest frame. A closer look, (Fig. 3b), indicates an excess of events near $2.4\,GeV$. An extra Gaussian was included to better fit the data. The fit (Fig. 3c) yielded 526 ± 65, 203 ± 60, and 211 ± 49 entries for the number of D_1^0, D_2^{*0} and the additional Gaussian combinations. The mass of the extra Gaussian was

$2398.1 \pm 2.1^{+1.6}_{-0.8} MeV$ with a width consistent with the detector resolution.

The ratios of the rates of the $D^{*\pm}\pi^{\mp}$ decay channel of D_1^0 and D_2^{*0} to $D^{*\pm}$ are $3.40 \pm 0.42^{+0.78}_{-0.63}\%$ and $1.37 \pm 0.40^{+0.96}_{-0.33}\%$, respectively. Extrapolating to the full kinematic region and using [13] along with known branching ratios [4] as well as isospin conservation, the result is given in table 1. This result is consistent with those from e^+e^- experiments.

TABLE 1. Comparison of D_1^0 and D_2^{*0} production rates. For ZEUS errors are statistical, systematic and extrapolation errors. For CLEO, OPAL and ALEPH the statistical and systematic errors have been added in quadrature. The DELPHI results are without systematic errors.

Experiment	$f(c \to D_1^0)$ [%]	$f(c \to D_2^{*0})$ [%]
ZEUS Prelim.	$1.46 \pm 0.18^{+0.33}_{-0.27} \pm 0.06$	$2.00 \pm 0.58^{+1.40}_{-0.48} \pm 0.41$
CLEO [15]	1.8 ± 0.3	1.9 ± 0.3
OPAL [16]	2.1 ± 0.8	5.2 ± 2.6
ALEPH Prelim. [17]	1.6 ± 0.5	4.7 ± 1.0
DELPHI Prelim. [18]	1.9 ± 0.4	4.7 ± 1.3

In order to search for a radially excited D^* meson, $D^{*'}$, the combination $M(K\pi\pi_s\pi_4\pi_5) - M(K\pi\pi_s) + M(D^*)$, where π_4 and π_5 are oppositely charged pions with $p_\perp > 0.125 GeV$, was fitted along with a background distribution of $x^\alpha e^{-\beta x}$, where $x = M(K\pi\pi_s\pi_4\pi_5) - M(K\pi\pi_s) - 2m_\pi$. No peak was seen in the expected mass range, $(2.59 - 2.67\, GeV)$ (Fig. 4). An upper limit was obtained by fitting

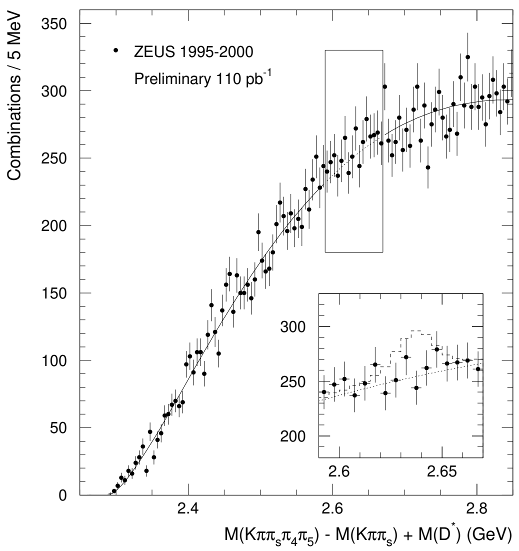

FIGURE 4. Distribution of $M(K\pi\pi_s\pi_4\pi_5) - M(K\pi\pi_s) + M(D^*)$ for the $D^{*\pm}$ candidates with the $D^{*'}$ window within the rectangle. Inset: Dashed histogram is the Monte Carlo signal normalized to the upper limit and added to the fit interpolation (dotted curve) in the $D^{*'}$ window.

the background outside this range, interpolating within the range and subtracting this from the data in the mass range. The 95% confidence level upper limit for the $D^{*\pm}\pi^+\pi^-$ decay relative to $D^{*\pm}$ was found to be 2.3%. Extrapolating to the full kinematic range and using [13], $f(c \to D^{*'+}) \cdot B_{D^{*'+} \to D^{*+}\pi^+\pi^-} < 0.7\%$ at 95% confidence level was obtained. The equivalent OPAL limit is 1.2% [8].

INELASTIC J/ψ PRODUCTION

The $\mu^+\mu^-$ decay channel of J/ψ for $0.4 < z < 0.9$, $50 < W_{\gamma p} < 180\,GeV$ and $Q^2 < 1\,GeV^2$, using the 1996-1997 data, has been studied [19]. Distributions in z, rapidity and transverse momentum squared of the J/ψ and a comparison with theoretical expectations are shown in Fig. 5. The z dependence of the data is not described in magnitude by the LO color singlet and octet model with octet matrix elements calculated from the CDF data [20,23]. On the other hand, the NLO color singlet model [21] roughly fits the spectrum for $p_{\perp\psi} > 1\,GeV$. For $p_{\perp\psi} > 2\,GeV$ the LO model with octet matrix elements from CLEO data agrees with the data for high z only [22,24]. Currently there is no calculation in NLO for the rapidity distribution. The NLO calculation agrees with the $p^2_{\perp\psi}$ data.

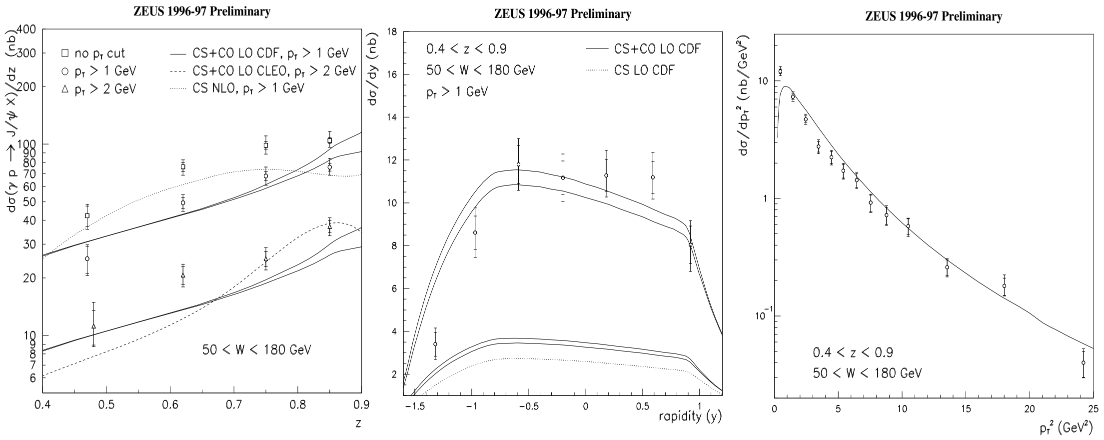

(a) (b) (c)

FIGURE 5. (a) z distribution for various $p_{\perp\psi}$ cuts: no cut (squares), $p_{\perp\psi} > 1\,GeV$ (circles) and $p_{\perp\psi} > 2\,GeV$ (triangles). Inner (outer) error bars are statistical (quadratic sum of statistical and systematic) errors. Lower pair of solid curves are a prediction of color singlet and octet model [20] for $p_{\perp\psi} > 1\,GeV$. Separation of the curves indicates the uncertainty in the color octet matrix elements. Upper pair of solid curves includes a scale factor of ~ 3. Dotted curve is the color singlet NLO prediction for the direct photon process and $p_{\perp\psi} > 1\,GeV$ [21]. Dashed curve is prediction of the color singlet and octet models for $p_{\perp\psi} > 2\,GeV$ [22]. (b) Rapidity distribution for $p_{\perp\psi} > 1\,GeV$. Solid curves as in (a). Dotted curve is the LO contribution of the direct photon color singlet component. (c) $p^2_{\perp\psi}$ distribution: Solid curve is the prediction of the NLO calculation [21].

REFERENCES

1. ZEUS Collaboration, Derrick M. et al., *Phys. Lett.* **B293**, 465 (1992). *The ZEUS Detector: Status Report 1993*,DESY 1993.
2. ZEUS Collaboration, Breitweg J. et al., *Phys. Lett.* **B481**, 213 (2000).
3. ZEUS Collaboration, Breitweg J. et al., *Eur. Phys. J.* **C6**, 67 (1999).
4. Caso C. et al., Particle Data Group, *Eur. Phys. J.* **C3**, 1 (1998).
5. Isgur N. and Wise M. B., *Phys. Lett.* **B232**, 113 (1989); Neubert N., *Phys. Reports.* **A245**, 259 (1994).
6. CLEO Collaboration, Anderson S. et al., *Nucl. Phys.* **A663**, 647 (2000).
7. DELPHI Collaboration, Abreu P. et al., *Phys. Lett.* **B426**, 231 (1998).
8. OPAL Collaboration, submitted to the XXIX International Conference on High Energy Physics, ICHEP 98, Vancouver Canada,July 1998; *OPAL PN*, 352.
9. CLEO Collaboration, Rodriquez J. L. *hep-ex.* **9901008**.
10. ZEUS Collaboration, Breitweg J. et al., *Z. Phys.* **C76**, 599 (1997); ZEUS Collaboration, contributed paper 814 to the XXIX ICHEP Conference, Vancouver, Canada (1998).
11. Jung H., Schuler A. and Terron J., ,*Int. Jour. of Mod. Phys.* **A7**, 7955 (1992).
12. Frixione S. et al., *Nucl. Phys.* **B454**, 3 (1995); *Phys. Lett* **B348**, 633 (1995).
13. Gladilin L., *hep-ex.* **9912064**.
14. ZEUS Collaboration, contributed paper 448 to the XXX ICHEP Conference, Osaka, Japan (2000).
15. CLEO Collaboration, Avery P. et al., *Phys. Lett.* **B331**, 236 (1994).
16. OPAL Collaboration, Ackerstaff K. et al., *Z. Phys.* **C76**, 425 (1997).
17. ALEPH Collaboration, *Production of D_1 and D_2^* mesons in hadronic Z decays*, Contributed paper to HEP99, Tampere, July 15-21, Abstract 5_411.
18. DELPHI Collaboration, *Narrow D^{**} production in c and b jets*, Contributed paper to ICHEP98, Vancouver, July 23-29, Paper 240.
19. ZEUS Collaboration, contributed paper 446 to the XXX ICHEP Conference, Osaka, Japan (2000).
20. Kniehl B. A. et al., *Eur. Phys. J.* **C6**, 493 (1999); Kniehl B. A., *Proceedings of the Workshop 1998-1999 on Monte Carlo Generators for HERA Physics*, ed. by Doyle A. T., Grindhammer G., Ingelman G. and Jung H., DESY-PROC-1999-02,p.427.
21. Kramer M. et al., *Phys. Lett.* **B348**, 657 (1995); Kramer M., *Nucl. Phys.* **B459**, 3 (1996).
22. Beneke M. et al., *hep-ex.* **0001062**, subitted to *Phys. Rev. D.*
23. CDF Collaboration, Abe F. et al., *Phys. Rev. Lett.* **79**, 578 (1997).
24. CLEO Collaboration, Balest R. et al., *Phys. Rev.* **D52**, 2661 (1995).